# IMECE2006-16063

# A DISTRIBUTED SENSING SYSTEM FOR VEHICLES STATE ESTIMATION

**Hamidreza Bolandhemmat**
PhD Student
Department of Mechanical Engineering
University of Waterloo
Waterloo, Ontario, Canada, N2L 3G1

**Christopher M. Clark**
Assistant Professor
Lab for Autonomous and Intelligent Robotics
Department of Mechanical Engineering
University of Waterloo
Waterloo, Ontario, Canada, N2L 3G1

**M. F. Golnaraghi**
Professor, Canada Research Chair
Mechatronics and Smart Materials Systems
Department of Mechanical Engineering
University of Waterloo
Waterloo, Ontario, Canada, N2L 3G1

## ABSTRACT

This paper presents the design of a distributed sensing system that uses an Extended Kalman Filter (EKF) to fuse measurements, so that automotive vehicle states can be estimated for use by a Semi-active Suspension control system. To improve ride comfort and handling quality, relative displacements and velocities of suspension systems are estimated. To control the stability of vehicles, roll, yaw, and pitch must also be determined. The designed (EKF) uses easily accessible measurements such as accelerations and body's angular velocities. These measurements are provided by 8 accelerometers and an Inertial Measurement Unit (IMU). The accelerometers are strategically mounted on the two ends of each individual shock absorber (damper). The IMU was mounted near the vehicle's center of gravity. Computer simulations and experiments were conducted for full vehicle state estimation of a 1993 Toyota Tercel equipped with the above mentioned sensor suite. Results show that except relative displacements, all states of the automobile's semi-active suspension systems can be estimated using this set of sensors. The designed EKF works well despite not knowing accurate information about road inputs, external disturbances and car characteristics such as moments of inertia, mass, and equivalent spring and damping coefficients. Both simulation results and experimental results show the effectiveness of the designed EKF in estimating the required states.

## INTRODUCTION

During last two decades, active suspension systems and semi-active dampers have been developed to improve performance parameters corresponding to terrain vehicles. Various types of controllers including linear/non-linear optimal and robust strategies have been proposed by researchers [1]. While active and semi-active damper technologies offer new opportunities to improve ride comfort, road handling and vehicle stability, the primary challenge of providing required control system feedbacks remains. Many proposed control laws have assumed that all the system states including suspension systems deflection and its rate, velocity of wheel hubs and tire deflections are completely and accurately measurable, which is not always the case [1- 5].

Velocity cannot be measured directly because velocity sensors must have a stationary reference space which is not applicable in automotive applications. Common techniques integrate accelerometer signals attached to the ends of each shock to achieve velocity information. Performance of low-cost automotive grade accelerometers is limited by high level noise (typically $50$-$1000\, \mu g / \sqrt{Hz}$ ) and drift due to biases and gravitational effects. Passing the integrated signal through a high-pass filter is not always adequate for obtaining accurate velocity data.

To make the various control methodologies realizable, a filter and/or observer is required to produce accurate state estimates. In [6] a modified Luenberger observer was presented to estimate semi-active suspension system states for a quarter

car model. In [7] and [8], an LQG/LQR method has been implemented to simultaneously observe and control states of an active suspension system in a half-car model. Despite the proven efficiency of the designed estimators in simulations, they use an incomplete vehicle model within the observers which can not capture full motion dynamics of a real vehicle [9]. In [10] and [11], a linear state observer has been utilized to implement the state feedback control law and a $H_2 / H_\infty$ performance based command, respectively, for active control of full car model (seven degree of freedom) suspension systems. The designed unbiased observer has been proven to be asymptotically stable, but it is not guaranteed to minimize estimation error covariance matrix. In [12], four quarter car model based Kalman Filters (KF) have been implemented to estimate active suspension system parameters of a military vehicle. The designed KF's are working based on preview information of the road. This information was provided by an optical preview sensor mounted in front of the vehicle. Sensor measurements are converted to road height by trigonometric equations. These preliminary computations need high processing power and time. Also, delays in providing road information may cause instability in integrated controller/observer system.

This paper proposes an appropriate sensory configuration to sense vehicle dynamics. The sensor set has been distributed strategically throughout the vehicle in order to capture sufficient information of the vehicle's behavior. An EKF has been developed to fuse sensors measurements to estimate the vehicle states required by Ride Handling and/or Stability Controllers (RHSC). Unlike previous research, the designed EKF benefits from states predicted by a full car (7DOF) kinematics /dynamics model of the vehicle. Also, the particular sensor configuration eliminates the need to evaluate road inputs. The content of the paper will be organized as follows. The next section considers the full car model. It describes the required modes of vehicle motion along with the particular state vector which has been defined for this application. Then, the sensor collection is introduced followed by simulation and experiment results of the designed EKF.

## 7 DOF VEHICLE DYNAMIC MODEL

The vertical dynamics of a vehicle include the four wheel bounce motions and the car body heave, roll, and pitch motions. This typical seven degree of freedom characterization is used for active and semi-active suspension systems design. Vertical and angular motion of the vehicle's body can be described by the following differential equations:

$$m\ddot{z}_{CG} = -k_{sF}(z_{CG} + b\phi - a\theta - z_1) - c_{LF}(\dot{z}_{CG} + b\dot{\phi} - a\dot{\theta} - \dot{z}_1) - k_{sR}(z_{CG} + b\phi + a\theta - z_2)$$
$$- c_{LR}(\dot{z}_{CG} + b\dot{\phi} + a\dot{\theta} - \dot{z}_2) - k_{sF}(z_{CG} - b\phi - a\theta - z_3) - c_{RF}(\dot{z}_{CG} - b\dot{\phi} - a\dot{\theta} - \dot{z}_3)$$
$$- k_{sR}(z_{CG} - b\phi + a\theta - z_4) - c_{RR}(\dot{z}_{CG} - b\dot{\phi} + a\dot{\theta} - \dot{z}_4)$$

$$(1)$$

$$I_{xx}\ddot{\varphi} = -bk_{sF}(z_{CG} + b\varphi - a\theta - z_1) - bc_{LF}(\dot{z}_{CG} + b\dot{\varphi} - a\dot{\theta} - \dot{z}_1) - bk_{sR}(z_{CG} + b\varphi + a\theta - z_2)$$
$$- bc_{LR}(\dot{z}_{CG} + b\dot{\varphi} + a\dot{\theta} - \dot{z}_2) + bk_{sF}(z_{CG} - b\varphi - a\theta - z_3) + bc_{RF}(\dot{z}_{CG} - b\dot{\varphi} - a\dot{\theta} - \dot{z}_3)$$
$$+ bk_{sR}(z_{CG} - b\varphi + a\theta - z_4) + bc_{RR}(\dot{z}_{CG} - b\dot{\varphi} + a\dot{\theta} - \dot{z}_4)$$

$$(2)$$

$$I_{yy}\ddot{\theta} = ak_{sF}(z_{CG} + b\varphi - a\theta - z_1) + ac_{LF}(\dot{z}_{CG} + b\dot{\varphi} - a\dot{\theta} - \dot{z}_1) - ak_{sR}(z_{CG} + b\varphi + a\theta - z_2)$$
$$- ac_{LR}(\dot{z}_{CG} + b\dot{\varphi} + a\dot{\theta} - \dot{z}_2) + ak_{sF}(z_{CG} - b\varphi - a\theta - z_3) + ac_{RF}(\dot{z}_{CG} - b\dot{\varphi} - a\dot{\theta} - \dot{z}_3)$$
$$- ak_{sR}(z_{CG} - b\varphi + a\theta - z_4) - ac_{RR}(\dot{z}_{CG} - b\dot{\varphi} + a\dot{\theta} - \dot{z}_4)$$

$$(3)$$

where $Z_{CG}$ is the heave displacement of the center of gravity of the body, $\varphi$ is the car body's bank angle, and $\theta$ is the pitch deflection. The vertical displacement of the Left-Front (LF), Left Rear (LR), Right Front (RF) and Right Rear (RR) wheels hubs are $Z_1$, $Z_2$, $Z_3$, and $Z_4$ respectively.
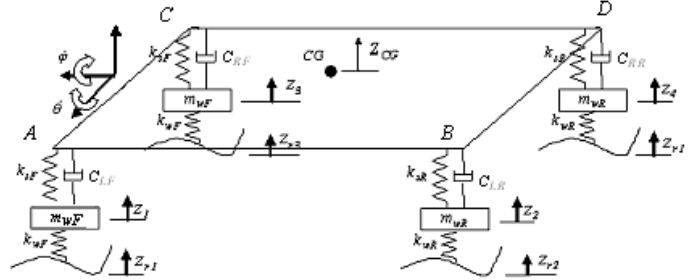


**Figure 1 Seven degrees of freedom vehicle model**

Differential equations govern vertical movement of the wheels are as follows

$$m_{wF}\ddot{z}_1 = k_{sF}(z_{CG} + b\varphi - a\theta - z_1) + c_{LF}(\dot{z}_{CG} + b\dot{\varphi} - a\dot{\theta} - \dot{z}_1) - k_{wF}(z_1 - z_{r1}) \quad (4)$$

$$m_{wR}\ddot{z}_2 = k_{sR}(z_{CG} + b\varphi + a\theta - z_2) + c_{LR}(\dot{z}_{CG} + b\dot{\varphi} + a\dot{\theta} - \dot{z}_2) - k_{wR}(z_2 - z_{r2}) \quad (5)$$

$$m_{wF}\ddot{z}_3 = k_{sF}(z_{CG} - b\varphi - a\theta - z_3) + c_{RF}(\dot{z}_{CG} - b\dot{\varphi} - a\dot{\theta} - \dot{z}_3) - k_{wF}(z_3 - z_{r3})$$

$$(6)$$

$$m_{wR}\ddot{z}_4 = k_{sR}(z_{CG} - b\varphi + a\theta - z_4) + c_{RR}(\dot{z}_{CG} - b\dot{\varphi} + a\dot{\theta} - \dot{z}_4) - k_{wR}(z_4 - z_{r4}) \quad (7)$$

States of the vehicle have been defined based on the particular application. Ride and Handling controllers usually need suspension and tire deflections from equilibrium as well as relative velocity of the suspension system and absolute velocity of unsprung masses. Also, angular velocity of the body and longitudinal/lateral accelerations of vehicle's center of mass should be provided for stability control systems. All of the required states except those corresponding to stability control are difficult to measure. Hence, they are selected as system states to be estimated by the EKF. The following state vector is introduced

$$\underline{x} = [x_1,...,x_{16}]^T \quad (8)$$

where $x_1$ to $x_8$ are relative displacement and velocity of each vehicle shock

$$x_1 = (z_{CG} + b\varphi - a\theta - z_1)$$
$$x_2 = (\dot{z}_{CG} + b\dot{\varphi} - a\dot{\theta} - \dot{z}_1)$$
$$x_3 = (z_{CG} + b\varphi + a\theta - z_2)$$
$$x_4 = (\dot{z}_{CG} + b\dot{\varphi} + a\dot{\theta} - \dot{z}_2)$$

$$x_5 = (z_{CG} + b\varphi - a\theta - z_3)$$
$$x_6 = (\dot{z}_{CG} + b\dot{\varphi} + a\dot{\theta} - \dot{z}_3)$$
$$x_7 = (z_{CG} - b\varphi + a\theta - z_4)$$
$$x_8 = (\dot{z}_{CG} - b\dot{\varphi} + a\dot{\theta} - \dot{z}_4)$$
$$(9)$$

and $x_9$ to $x_{16}$ are deflections and absolute velocities of each wheel

$$x_9 = (z_1 - z_{r1})$$
$$x_{10} = \dot{z}_1$$
$$x_{11} = (z_2 - z_{r2})$$
$$x_{12} = \dot{z}_2$$
$$x_{13} = (z_3 - z_{r3})$$
$$x_{14} = \dot{z}_3$$
$$x_{15} = (z_4 - z_{r4})$$
$$x_{16} = \dot{z}_4$$
$$(10)$$

In equation (10), the road profile at each wheel is represented by $z_{ri}$'s with $i = 1,2,3$ and $4$. Having obtained the above sets of states, vehicle dynamics can be expressed in the following state space form:

$$\underline{\dot{x}} = A\underline{x} + B\underline{u} + L\underline{w} \qquad (11)$$

where $\underline{u}$ is the input vector

$$\underline{u} = [\dot{z}_{r1}, \dot{z}_{r2}, \dot{z}_{r3}, \dot{z}_{r4}]^T \qquad (12)$$

and $\underline{w}$ denotes external disturbance exerted to the system. It is assumed to be white noise with its power demonstrating the level of confidence respect to the given model.

## SENSORS/KINEMATIC MODEL INTEGRATION USING EKF

### Sensors configuration

The sensor configuration should be capable of providing enough information about each wheel's motion as well as the car body's dynamic behavior. Since relative velocity suspension systems and absolute velocity of each hub are importance for RSC's, two accelerometers are suggested to be installed at the ends of each automobile damper, (i.e. eight total). In addition, sensors mounted at each wheel hub provide the estimator sufficient information about the road disturbances. An IMU mounted close to vehicle's center of mass is also proposed to capture angular motion of the body as well as lateral acceleration of the CG for feedback to the stability controller. It should be noted that vertical acceleration of the CG has been utilized by some researchers as a key parameter in optimal ride control systems [7].
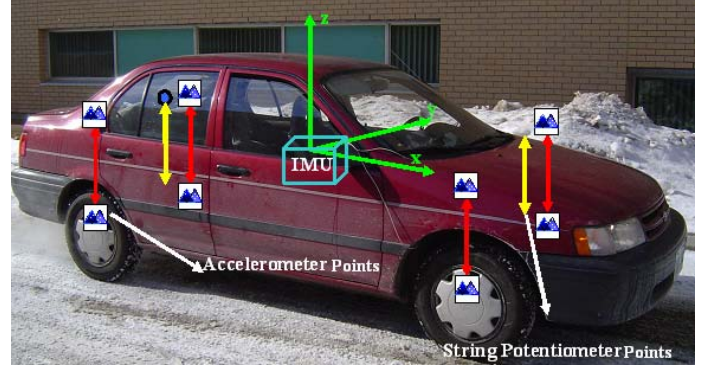


**Figure 2 Configuration of sensors and IMU mounted on the vehicle**

Figure 2 shows the Toyota Tercel with 8 MechSenseTM MD S 202 –U accelerometers mounted on the both ends of the shock absorbers (dampers) of each suspension system. A MechSense IMU was also installed near the center of gravity. Two string potentiometers Model # 0173-0161 were also mounted on the left front and rear suspensions. The displacement sensors are used only as a research tool to provide truth data of the actual displacements.



**Figure 3 Accelerometer mounted on the bottom of a damper to measure the vertical acceleration of the wheel hub**

Table 1 provides important specifications of the accelerometers and IMU sensors. The complete information can be found in corresponding data sheets [13]. Furthermore, the outputs of all sensors sampled at a rate of 1000 HZ at 12 bit resolution are sent through an RS232 level serial interface to an onboard computer. Figures 3 shows an accelerometer mounted to the wheel end of the left front suspension system of the Tercel.

| Gyroscopes | |
|---|---|
| Scale Factor Error | $0.1\% \, FS$ |
| Noise Density | $0.05 \, \text{deg/sec/} \sqrt{Hz}$ |
| Linear Acceleration Effect | $0.2 \, \text{deg/sec/g}$ |
| Bandwidth | 40HZ |
| Accelerometers | |
| Scale Factor Error | $0.3\% \, FS$ |
| Noise Density | $200\text{-}1000 \, \mu g / \sqrt{Hz}$ |
| Bandwidth | 50HZ |

**Table 1 Specification of the individual sensors**

Having considered the aforementioned sensory collection, the measurement model of the system can be described as a nonlinear combination of the predefined sixteen states as follows:

$$\underline{z}_k = h(\underline{x}[k], k) + \underline{v}_k \qquad (13)$$

with measurement vector

$$\underline{z}_k = [a_{CG}, \dot{\varphi}, \dot{\theta}, a_A, a_B, a_C, a_D, a_{wh1}, a_{wh2}, a_{wh3}, a_{wh4}]^T \quad (14)$$

and elements of the non-linear function $h$ are as follows

$$h(1) = \ddot{z}_{CG}$$
$$h(2) = (x_2 - x_6 + x_{10} - x_{14}) / 2b$$
$$h(3) = (-x_2 + x_4 - x_{10} + x_{12}) / 2a \qquad (15)$$

Acceleration of each corner of the car body can be related to acceleration of the CG applying Coriolis law

$$\underline{a}_i^B = \underline{a}_{CG}^B + \underline{\omega}^B \times (\underline{\omega}^B \times \underline{r}_i^B) + \underline{\alpha}^B \times \underline{r}_i^B \qquad (16)$$

Superscript $B$ denotes vectors have been expressed in body reference frame of the vehicle centered at CG. $\underline{r}_i^B$ with $i = A, B, C \text{ and } D$ is the coordination vector of each body corner in body reference frame (see Figure 1). Also, angular acceleration of the vehicle in body frame is

$$\underline{\omega}^B = [\dot{\phi}, \dot{\theta}, \dot{\psi}]^T$$
$$\underline{\alpha}^B = [\ddot{\phi}, \ddot{\theta}, \ddot{\psi}]^T \qquad (17)$$

Assuming negligible yaw motion of the vehicle, after some mathematical manipulation, acceleration of body ends of each damper can be described as

$$h(4) = \ddot{z}_{CG} - (\dot{\phi}^2 + \dot{\theta}^2)h - a\ddot{\theta} + b\ddot{\phi}$$
$$h(5) = \ddot{z}_{CG} - (\dot{\phi}^2 + \dot{\theta}^2)h + a\ddot{\theta} + b\ddot{\phi}$$
$$h(6) = \ddot{z}_{CG} - (\dot{\phi}^2 + \dot{\theta}^2)h - a\ddot{\theta} - b\ddot{\phi}$$
$$h(7) = \ddot{z}_{CG} - (\dot{\phi}^2 + \dot{\theta}^2)h + a\ddot{\theta} - b\ddot{\phi} \qquad (18)$$

and signal of the accelerometers attached to each wheel hub are given by equation (13)

$$h(8) = \ddot{z}_1$$
$$h(9) = \ddot{z}_2$$
$$h(10) = \ddot{z}_3$$
$$h(11) = \ddot{z}_4 \qquad (19)$$

The measurement noise $\underline{v}_k$ is assumed to be zero-mean Gaussian noise with covariance $R_k$. The power matrix of the measurement noise is determined based on the sensor characteristics given in table 1.

**Discrete EKF structure**

The EKF works on a prediction-correction basis. First, it makes a prediction using previous states and the 7DOF car model. Then, the predicted states of the vehicle are updated incorporating 8 accelerometer and IMU signals. Available information weighted by their confidence level are incorporated together to get the most reliable and accurate vehicle states. The measurement update is generally given by [14]

$$\hat{\underline{x}}_k(+) = \hat{\underline{x}}_k(-) + K_k(\underline{z}_k - h(\hat{\underline{x}}_k(-))) \qquad (20)$$

$K_k$ is the Kalman gain and described by

$$K_k = P_k(-)H_k^T[H_k P_k(-)H_k^T + R_k]^{-1} \qquad (21)$$

In the above equation, matrix $H_k$ is a Jacobian resulting from the Taylor series expansion evaluated at the prior estimate of the system state at $t = k$,

$$H_k = \left. \frac{\partial h(\underline{x}[k], k)}{\partial \underline{x}[k]} \right|_{\underline{x}[k] = \underline{x}_k(-)} \qquad (22)$$

The estimation error covariance matrix is corrected by modified formula which reduces the probability that the error covariance matrix becomes negative definite

$$P_k(+) = (I - K_k H_k)P_k(-)(I - K_k H_k)^T + K_k R_k K_k^T \qquad (23)$$

Between measurements a discrete model of the sampled data system can be used to propagate the estimated states. The above mentioned model digitized by a zero-order hold can be written as

$$\hat{\underline{x}}_{k+1}(-) = \Phi(k+1, k)\hat{\underline{x}}_k(+) + B_d \underline{u}_k + \underline{w}_k \qquad (24)$$

where state transition matrix is the following exponential series

$$\Phi(k+1, k) = \exp(A\Delta T) \qquad (25)$$

and input matrix becomes [15]

$$B_d = \int_0^{\Delta T} e^{A\xi} B d\xi = \sum \frac{A^k \Delta T^{k+1}}{(k+1) \, I} \qquad (26)$$

The error covariance matrix is propagated between measurements applying the following equality

$$P_{k+1}(-) = \Phi(k+1, k)P_k(+)\Phi(k+1, k)^T + Q_k \qquad (27)$$

$Q_k$ is the power of the discrete process noise and is related to the continuous process white noise covariance matrix by the equation (28)

$$Q_k = \int_{t_k}^{t_{k+1}} \Phi(\tau, k)Q(t)\Phi(\tau, k)^T d\tau$$

$$E\left\langle \underline{w}_k \underline{w}_k^T \right\rangle = Q_k \qquad (28)$$

The EKF structure described by equations (20) to (28) is then applied to state estimation of the aforementioned 7DOF full car system.

## State estimation of the 7DOF car model

### Simulation Results

Computer simulation of the designed EKF was performed for two different situations. The first EKF deals with a non-linear time varying dynamic system which receives damping coefficient feedback from a semi-active suspension controller. The controller adjusts the damping values in order to improve ride and handling performance of the Tercel. In the second situation, damping coefficients of the semi-active suspension systems remain constant. Simulations of the first situation demonstrate the EKF's ability to handle uncertain time varying dynamics. Simulations of the second situation illustrates that even in a time invariant system, relative displacement states are not observable. Both simulation situations utilize equation (11) as process dynamics and (13) as the measurement system model. For both cases, the road input to the 7DOF car model is a sinusoidal signal with frequency of $5\,rad/\sec$ and amplitude of $0.15\,m$.
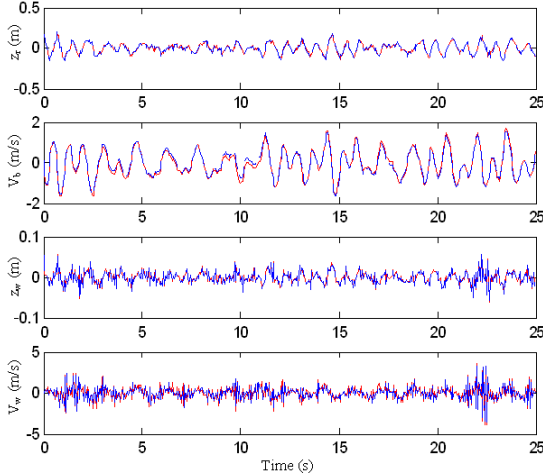


**Figure 4 Estimated [Blue] and actual states [Red] of the LF suspension system (controlled semi-active suspension system)**

All parameters in 7DOF car model have been set based on Toyota Tercel Specifications (see the appendix). Figure 4 compares the designed EKF estimation results and actual states of vehicle LF suspension system. These states are relative displacement and velocity of the shock, absolute velocity of wheel hub and tire deflection. It is evident that the EKF can effectively estimate the aforementioned states.
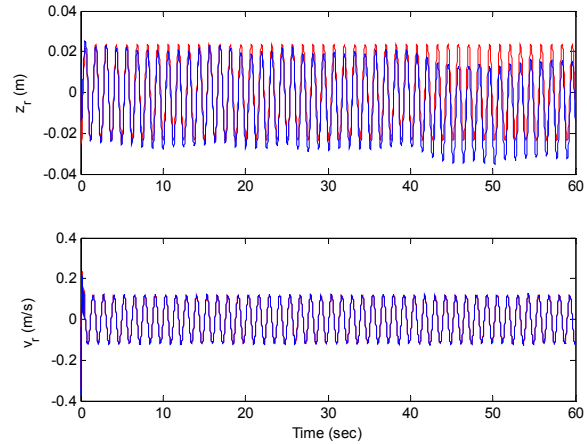


**Figure 5 Actual relative displacement and velocity [red] of the LF suspension system with their estimations [blue] (uncontrolled semi-active system)**

Simulation results of the second situation are given in Figure 5 and 6. The simulation time has been extended to 60 seconds in order to illustrate quick degradation in relative displacement and tire deflection estimations. This happens for all four suspension systems. It should be noted that suspension system relative velocity and absolute velocity of the wheel hub remain accurate. It suggests that the proposed sensor configuration would be suited for control applications which rely on relative deflection information of vehicle suspension systems.
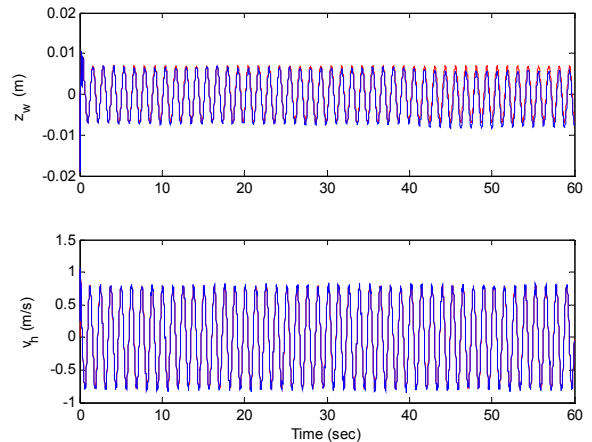


**Figure 6 Actual Tire Deflection and Wheel hub Velocity [red] of the LF suspension system with their estimations [blue]**

Figure 7 illustrates estimation errors and their corresponded variances reported by EKF. It demonstrates that with time increasing, the EKF confidence to the estimated relative displacement state is decreased. It is obvious that the variance related to relative velocity estimation error remains constant. Figure 7 also zoomed on the first 20 seconds to imply

how much fast only with 2 or 3 iterations the EKF estimated states converge to the actual vehicle states.
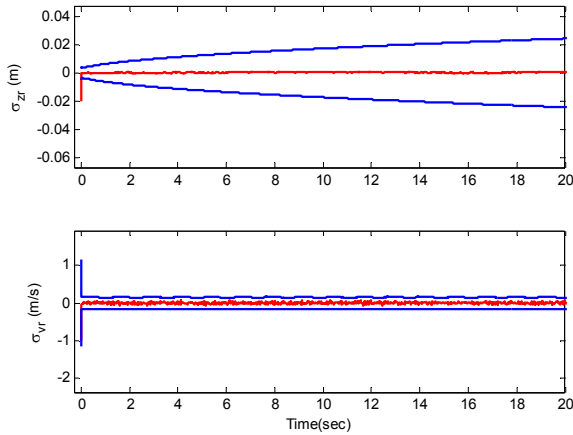


**Figure 7 The graph illustrates relative displacement and velocity estimation error variances +/-σ for the LF suspension system.**

## Experimental Results

In order to validate the EKF, the Tercel was driven with a speed 30 $km/h$ over a road with a hole, bump, and also smooth sections as shown in figure 8. Sensor data including eight accelerometers, an IMU were stored at sampling rate of 2 ms.
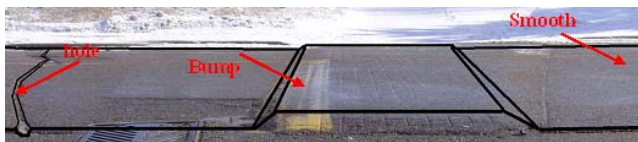


**Figure 8 Bump (Road Ring, University of Waterloo)**

As shown in the Figure 9 to 12, EKF can effectively estimate all of the states of the LF suspension system. The figures have been zoomed on the time segment for which the car passes over the hole and bump to clarify the effectiveness of estimation process. However, it has been demonstrated that estimation error corresponded to relative displacement would gradually grow (see Figure 5 and 7). It also should be mentioned that when the suspension system is compressed, the string potentiometer can not capture the relative displacement. Therefore, truth data in negative displacement regions of Figures 9 is unreliable.
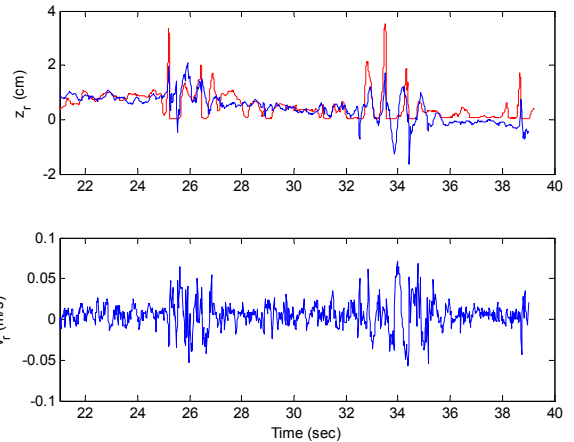


**Figure 9 The graph compares the LF suspension system true relative displacement [red] with their estimations [blue]**

Road input is provided by appropriately filtering a white noise. The following first order shape filter with appropriate bandwidth has been used to provide $u$ in equation (12)

$$F_{SF} = \frac{\alpha_{SF}}{s + \beta_{SF}} \tag{29}$$

The bandwidth and DC value of the shape filter were selected to be able to mimic the road profiles of 4-12cm height and with vehicle velocities within 25-45 $km/h$. Road input uncertainties were partially compensated in the process noise power.
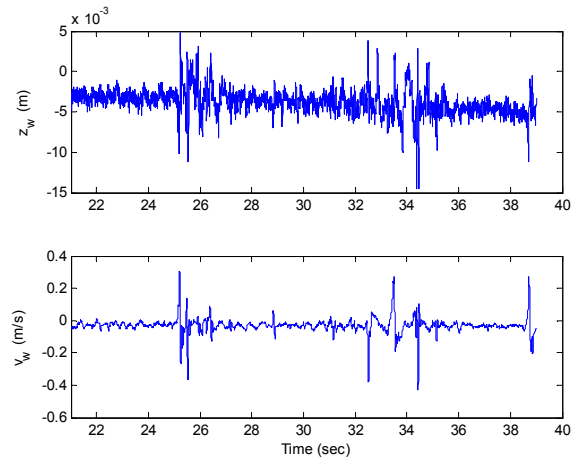


**Figure 10 The graphs estimate the tire deflection and velocity of the wheel hub for LF wheel**

Measurement residuals (or innovation) obtained by comparing the filter outputs to the measurements at each time step are given in figures 11 and 12. Consistency between the residuals and their expected covariance bands is interpreted as the best reliability indicator of EKF's. Assuming Ergotic properties for the innovation and that the process and

measurement noises are uncorrelated, the measurement residual covariance and average can be expressed as

$$E\left\langle (\underline{z}-\hat{\underline{z}})(\underline{z}-\hat{\underline{z}})^T \right\rangle = H_k P_k(-)H_k^T + R_k \qquad (30)$$

$$E\left\langle (\underline{z}-\hat{\underline{z}}) \right\rangle = 0 \qquad (31)$$

where $\underline{z}$ is the actual measurement vector captured from the aforementioned eleven sensors and $\hat{\underline{z}}$ is the estimated measurement vector by the EKF.
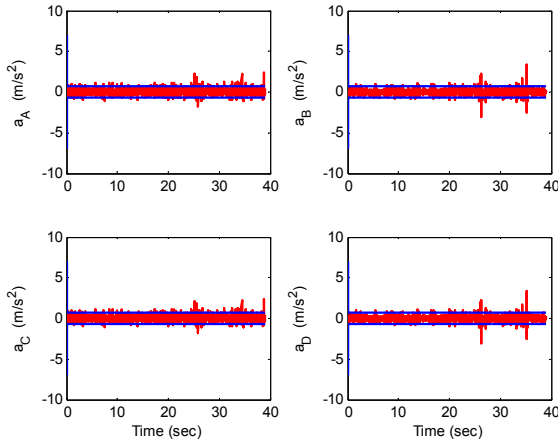


**Figure 11 The graph illustrates innovation signal corresponded to accelerations of four corner of the car body [red]. Blue curves are expected variance +/-σ of each residual.**

Figure 11 compares EKF residuals corresponding to each accelerometer signal attached to Tercel body corners (points $A, B, C$ and $D$, see figure 1) and the expected variances from equation (30). The same scenario has been depicted in figure 12 for signals of the accelerometers mounted on each wheel hub. It can be seen that the variances of measurement residuals are similar to the EKF predictions. It is also obvious that measurement residuals have expected values of zero to satisfy equation (31). Finally, it demonstrates that the measurement model and the covariance matrix of the measurement vector have been selected properly.
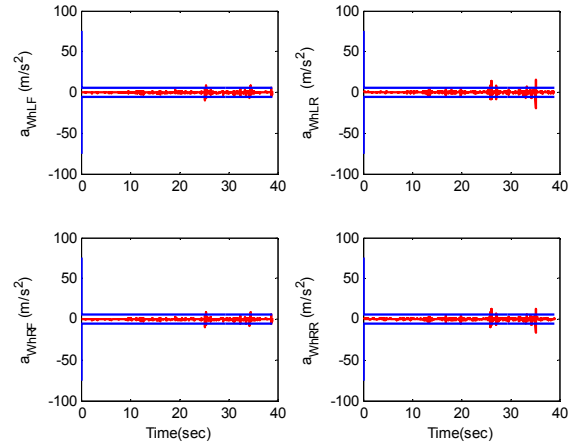


**Figure 12 The graph illustrates innovation signal corresponded to each accelerometer attached to each wheel [red]. Blue curves are expected variance +/-σ of the residuals.**

## CONCLUSION

The paper proposed a distributed sensors system in order to capture vehicle dynamic behavior. Eight accelerometers were proposed to be installed, with two at each end of a suspension system. The accelerometers can provide rich information of vehicle suspension systems as well as road profiles. An IMU close to vehicle CG is also suggested to measure angular motion of the car and provide lateral acceleration to be used by stability controllers.

An EKF was designed to incorporate all sensors signals and a full car kinematics model to estimate the states required by the RHSC's. Both simulation and experimental results demonstrate that the proposed sensors configuration with a 7DOF car model can provide enough information to estimate relative velocity and absolute velocity states with sufficient accuracy. Also, based on the results relative displacement states are not observable using the aforementioned sensors set. Fortunately, all of the practical Ride and handling controllers rely on relative and absolute velocity states and acceleration of ends of suspension systems. Future work will minimize the number of sensors with maintaining the EKF estimation quality. Also, studies into incorporating vehicle dynamic lateral modes into the EKF will be carried out to estimate tire friction forces as well as tire sideslip angle which are feedbacks of the ABS and traction control systems.

## REFERENCES

[1] Hrovat, D., "Survey of advanced suspension developments and related optimal control applications", Automatica, 33(10), pp.1781-1787, 1997.

[2] Hrovat, D., Margolis, D. L., and Hubbard, M., "An Approach toward the Optimal Semi-active Suspensions". ASME Journal of Dynamic Systems, Measurement, and Control, Vol. 110, No. 3, 1988, pp.288-296.

[3] Margoils, D., "The Response of Active and Semi-active Suspensions to Realistic Feedback Signals", Vehicle System Dynamics, Vol. 12, 1983, pp. 317-330.

[4] N. Al-Holou, D. S. Joo, A. Shaout, "The development of Fuzzy Logic Based Controller for Semi- Active Suspension Systems", Proceeding of the 37th Midwest Symposium on Circuits and Systems, IEEE, pp. 1373-1376, 1996.

[5] Irmscher, S. and Hees, E., "Experience in Semi-active Damping with State Estimators", proceeding of AVEC 96, International Symposium on Advanced Vehicle Control, Aachen University of Technology, June 1996, pp. 193-206.

[6] YI, K. and Song, B. S., "Observer Design for Semi-Active Suspension Control", Vehicle System Dynamics, 32 (1999), pp.129-148.

[7] Taghirad, H. and Esmailzade, E., "Automotive passenger Comfort Assured through LQG/LQR Active Suspension", Journal of Vibration and Control, 1997.

[8] Roh, H. S. and Park, Y., "Stochastic Optimal Preview Control an Active Vehicle suspension", Journal of Sound and Vibration 220(2), 313-330, 1999.

[9] C. Clark, Hamidreza Bolandhemmat, Project #: 3780601, Phase 1, MMO Report, "Ride and Stability Controller and Integrated Sensor System", Mechanical Engineering Department, University of Waterloo, 2006.

[10] E. Esmailzadeh, H. Bateni, "Optimal active suspensions with full state feedback control", SAE Transactions, Journal of Commercial Vehicles, 101:784-79,1992.

[11] Lu, J. and DePoyster, M., "Multiobjective Optimal Suspension Control to Achieve Integrated Ride and Handling Performance", IEEE Transaction on Control, systems Technology, Vol. 10, NO.6, November 2002.

[12] Donahue, M. D., Hedrick, J. K., "Implementation of an Active Suspension, Preview Controller for Improved Ride Comfort".

[13] MechSenseTM MD S 202 –U and MechSenseTM IMU data sheet.

[14] A. H. Jazwinski, "Stochastic processes and Filtering Theory", Academic Press, 1970.

[15] A. Gelb, "applied Optimal Estimation", Fifth edition, 1999.

## NOMENCLATURE

$I_{xx} = 423\,kgm^2$ Car body moment of inertia around its longitudinal axis

$I_{yy} = 1537\,kgm^2$ Car body moment of inertia around its lateral axis

$a = 1.25\,m$ Half of the distance within two suspension system along x axis

$b = 0.6\,m$ Half of the distance within two suspension system along y axis

$h = 0.25\,m$ Height of each corner of the car body above the CG along z direction

$m = 1361.7\,kg$ Mass of the car body

$m_{wF} = 50\,kg$ Mass of front wheels

$m_{wR} = 50\,kg$ Mass of Rear wheels

$C_{LF} = 10162\,N\sec/m$ Nominal Damping coefficient of Left Front suspension system

$C_{LR} = 10162\,N\sec/m$ Nominal Damping coefficient of Left Rear suspension system

$C_{RF} = 10162\,N\sec/m$ Nominal Damping coefficient of Right Front suspension system

$C_{RR} = 10162\,N\sec/m$ Nominal Damping coefficient of Right Rear suspension system

$k_{sF} = 27000\,N/m$ Spring coefficient of front suspension systems

$k_{sR} = 27000\,N/m$ Spring coefficient of rear suspension systems

$k_{wF} = 150420\,N/m$ Front tires spring coefficient

$k_{wR} = 150420\,N/m$ Rear tire spring coefficient

$\hat{\underline{x}}_k(+)$ Updated estimate of the system state at $k^{th}$ step

$\hat{\underline{x}}_k(-)$ Predicted estimate of the system state at $k^{th}$ step

$P_k(-)$ Updated estimation error covariance matrix at $k^{th}$ step

$P_k(+)$ Predicted estimation error covariance matrix at $k^{th}$ step

$\beta_{SF}$ Bandwidth of the shape filter

$\dfrac{\alpha_{SF}}{\beta_{SF}}$ DC value of the shape filter